



Supplementary Information for

Solar Driven, Highly Sustained Splitting of Seawater into Hydrogen and Oxygen Fuels

Yun Kuang, Michael J. Kenney, Yongtao Meng, Wei-Hsuan Hung, Yijin Liu, Jianan Erick Huang, Rohit Prasanna, Pengsong Li, Yaping Li, Lei Wang, Mengchang Lin, Michael D. McGehee, Xiaoming Sun and Hongjie Dai

Hongjie Dai and Xiaoming Sun

Email: hdai@stanford.edu, sunxm@mail.buct.edu.cn

This PDF file includes:

Supplementary text
Figs. S1 to Sx
Caption for movies S1
References for SI reference citations

Other supplementary materials for this manuscript include the following:

Movies S1

Supplementary Information Text

Materials and Methods

Formation of NiS_x-Ni foam: Ni foam (420 g/m², degreased via sonication in acetone and ethanol) were first annealed at 500 °C in 10% H₂ (by volume, 90% Ar) atmosphere to fully remove the surface native oxide layer. 50 mg of sulfur powder (Sublimed, JT Baker) were dissolved in 30 mL of anhydrous toluene (Sigma-Aldrich, 99.9%) in a Teflon-lined stainless-steel autoclave. Then two pieces of the as annealed Ni foam with a size of 1cm * 3.5 cm were placed in the toluene solution. The autoclave was then heated to 150 °C for 5 hours. After the autoclave was allowed to cool to room temperature, the product was washed 3 times with ethanol and toluene and dried at room temperature.

Electrodeposition of NiFe to form Ni³⁺: Ni foam (420 g/m², degreased via sonication in acetone and ethanol) or NiS_x-Ni foam were placed in a 150 mL solution of 6 mM Ni(NO₃)₂ (Sigma-Aldrich, 98%) with 2 mM Fe(NO₃)₃ (Sigma-Aldrich, 98%) as the working electrode with Pt mesh (counter) and Ag/AgCl satd. KCl (reference). The solution was kept at 10 °C by ice bath and stirred at 100 rpm. The working electrode was held at -1 V vs. Ag/AgCl satd. KCl (R = 20 Ω) for 45 minutes and a hydroxide layer was formed. The electrode was rinsed with deionized water and then dried at room temperature.

Formation of Ni-NiO-Cr₂O₃ cathode follows our previous work(1) with slight changes. In a typical synthesis, 0.8 mL of 0.2 M Ni(CH₃COO)₂ (Sigma-Aldrich, 98%) and 40 μL of 0.5 M Cr(NO₃)₃ (Sigma-Aldrich, 99.99%) were added to 8 mL of anhydrous N,N-dimethylformamide (Acros, 99.8%) in a 20 mL scintillation vial and stirred vigorously at 90 °C for 4 hours. After stirring, the product was collected and washed with ethanol (Fisher, Histological grade) 3 times via centrifugation. The product was re-dispersed in ethanol and sonicated with 30 wt% 20 nm Ni particles (US Research Nanomaterials, 99.9%) for 30 minutes. The dispersion was then loaded into Ni foam (420 g/m², degreased via sonication in acetone and ethanol) at 90 °C and then annealed in a vacuum furnace under Ar flow (1.5 Torr) for 1 h at 300 °C. The weight difference between the bare foam and the foam after annealing was taken to be the catalyst loading. One 8 mL of N,N-DMF will produce an electrode with 8 mg/cm² Ni-NiO-Cr₂O₃ + 30 wt% 20 nm Ni. For our study, we used double loading (16 mg/cm² Ni-NiO-Cr₂O₃ + 30 wt% 20 nm Ni) to improve performance at high current.

Perovskite solar cell fabrication: The perovskite precursor solution for making solar cells was prepared by dissolving appropriate ratios of Formamidinium Iodide (Dyesol), Caesium Iodide (Sigma Aldrich), Lead (II) Bromide (TCI), and Lead (II) Iodide (TCI), in a mixed solvent comprising 80% N,N-dimethylformamide (DMF, Sigma Aldrich) and 20% Dimethylsulfoxide (DMSO, Sigma Aldrich) by volume, at 1.0 M concentration. The perovskite composition used was $\text{FA}_{0.83}\text{Cs}_{0.17}\text{Pb}(\text{I}_{0.83}\text{Br}_{0.17})_3$.

The perovskite solar cells were fabricated using a procedure adapted from our previous work.⁽²⁾ ITO-coated glass substrates (10 ohm/sq, Xin Yan technologies) were cleaned by sonication in Extran detergent, acetone, and isopropyl alcohol, followed by UV-ozone treatment for approximately fifteen minutes. A solution of PTAA (Poly[bis(4-phenyl)(2,4,6-trimethylphenyl)amine]) (5 mg/mL in chlorobenzene, PTAA from Solaris) was spin coated on the ITO at 4000 RPM for 45 s as the hole transport layer. The perovskite solution was then spin-coated using the following spin procedure - 1000 RPM 10 s (1000 RPM/s acceleration), followed by 6000 RPM for 25 s (6000 RPM/s acceleration), and 1000 RPM for a further 5 s. During the last five seconds, compressed nitrogen (at 40 PSI) was blown directly on the spinning sample. Immediately after the spin, the film was annealed at 60 C for 3 s, followed by 105 C for 30 min. Following perovskite deposition, 40 nm of C_{60} (MER Corporation, 99.9% sublimed grade) and 8 nm of Bathocuproine (TCI) were deposited by thermal evaporation, followed by 130 nm of silver (Kurt J. Lesker) through a shadow mask, also by thermal evaporation. All fabrication was conducted in a nitrogen filled glovebox.

The solar cells were tested in ambient air under an Oriel solar simulator with a Xenon lamp calibrated to 1 sun intensity by measuring current in an NREL-certified KG5-filtered silicon photodiode. A Keithley 2400 source measure unit was used to record JV curves. The External Quantum Efficiency spectrum was measured using monochromated illumination from a Xenon lamp chopped at 73 Hz, with SR-830 lockin amplifiers used to measure currents in the solar cell and in a reference photodiode. A homebuilt maximum power point tracking program was used to measure stabilized efficiency of the solar cell.

Electrochemical experiments:

Ni³⁺ Anode activation/passivation preparation: The as-fabricated seawater splitting anodes were clamped by a Teflon-covered platinum electrode holder to make electrical contact. In order to avoid salt accumulation on the electrolyte/electrode/air interface during electrolysis in salty electrolyte, the as prepared electrodes were sealed by epoxy (Loctite EA 1C) with 1cm*1cm anode materials exposed to the electrolyte (or 0.5cm², 0.25cm² mentioned in the figures). Before seawater splitting and oxygen evolution reaction (OER) tests, all the anodes were activated in 1 M KOH (Sigma-Aldrich, ACS Reagent >85%) at a constant anodic current density of 100 or 400 mA/cm² for 12 h and then in 1 M KOH +

0.5 M (or 1 M, 1.5 M, 2 M, same salt concentration as in the stability test) NaCl (Sigma-Aldrich, 99%) electrolytes, as described in the captions of the figures.

Oxygen evolution reaction (OER) studies were carried out in a standard three-electrode system controlled by a CHI 760D electrochemistry workstation. The as-fabricated anodes were used as working electrodes, Pt mesh and saturated calomel electrode (SCE) were used as the counter and reference electrode, respectively. The reference was calibrated against and converted to reversible hydrogen electrode (RHE) by zero current potential of Pt mesh during the CV scans (0.5 mV/s) around HER onset range in a hydrogen-saturated electrolyte. Linear sweep voltammetry was carried out at 1 mV/s between 1 V and 1.8 V (vs. RHE) for the polarization curves. The anodes were cycled ~50 times by cyclic voltammetry (CV) until a stable CV curve was developed before measuring polarization curves. All polarization curves were not iR-compensated.

Seawater electrolysis were carried out on a LANHE battery tester working at constant charging mode with a constant current density. The as prepared Ni³ foam (or other anode samples prepared) were used as anodes and Ni-NiO-Cr₂O₃ was used as cathode. Quartz cell was used for 1M KOH room temperature test, and Teflon cell was used for 6M 80C test. Certain amount of deionized water was added every day to make sure the volume of the electrolytes were 100 mL. Note, all the Ni³ anodes were activated first and then were rinsed with deionized before pairing with new Ni-NiO-Cr₂O₃ cathodes for stability tests. In addition, a fresh electrolyte was used for two electrode stability test. This was because activation of Ni³ would oxidize and dissolve some NiS_x into the electrolyte, and these dissolved materials might be reduced or deposited on the cathode during long term electrolysis, thus would poison the Ni-NiO-Cr₂O₃.

Solar-cell-driven electrolysis measurement: To measure the efficiency of electrolysis driven by the perovskite solar cells, two solar cells in series (each with total area 0.2 cm², and masked area 0.12 cm²) were connected with the electrolyzer (anode and cathode each with a geometrical area of 1 cm²). Prior to electrolysis with the solar cell, the anode was activated vs. a Pt mesh electrode (400 mA/cm² in 1 M KOH for 12 h followed by 100 mA/cm² in 1 M KOH + 0.5 M NaCl for 12 h), rinsed with water and paired with a fresh Ni-NiO-Cr₂O₃. The electrolyzer was operated at 20 mA/cm² to verify stable performance before being paired with the solar cell tandem. A Keithley 2400, also connected in series, was used to measure current driven in the circuit. The solar to hydrogen efficiency (STH) was calculated according to the following equation:(3)

$$\text{STH}\% = (j \cdot 1.23 \text{ V}) / 100 \text{ mW/cm}^2 * 100$$

Commercial Si solar cell (Renogy E.Flex 5W, 5 V 1 A, item model number: RNG-CMP-EFL5-B) was purchased from Amazon.com, the solar driven high current electrolysis test was performed by connecting the Si solar cell to the electrolyzer (anode and cathode each

with a geometrical area of 1 cm²) under sunlight. The current and voltage were measured by a multimeter.

Gas Chromatography measurement: OER tests were performed in a gas-tight electrochemical cell with 1 M KOH or 1 M KOH + 0.5/1/1.5/2 M NaCl electrolyte and SCE reference electrode. Chronopotentiometry was applied with different current densities to maintain constant oxygen generation. Meanwhile, Ar was constantly purged into the anodic compartment with a flow rate of 25 cm³/min and the compartment was connected to the gas-sampling loop of a gas chromatograph (SRI 8610C). A thermal conductivity detector (TCD) was used to detect and quantify the oxygen generated.

Materials Characterization:

The size and morphology of the samples were characterized using a field-emission scanning electron microscope (SEM) (JEOL JSM6335) operating at 20 kV. Cross sectional, elemental mapping was performed using a focused ion beam (FIB)-SEM instrument (FEI Helios NanoLab 460 HP). Transmission electron microscopy (TEM) measurements and electron diffractions were carried out using a JEOL JEM 2100 system operating at 200 kV. Raman spectroscopy was carried out using a Horiba raman spectrometer equipped with an Olympus BX41 microscope and a Spectra-Physics 532 nm Ar laser.

X-ray spectroscopy:

X-ray micro tomography was conducted using both synchrotron (beamline 2-2 of Stanford Synchrotron Radiation Lightsource) and laboratory (Stanford Nano Shared Facilities) based X-ray sources. High energy X-rays penetrate through the sample and are converted into visible photons by a scintillator crystal before the transmission images are recorded using a 2D area detector. Samples are rotated along a vertical axis with an angular step of 0.5 degrees to facilitate the tomographic reconstruction. Our micro tomographic scans generate data with 3D spatial resolution at ~1 micron, which is sufficient for resolving the morphology of the metal foams.

Time-of-Flight Secondary Ion Mass Spectrometry (TOF-SIMS) mapping:

TOF-SIMS were performed with a PHI TRIFT V nanoToF (Chigasaki, Japan) ToF-SIMS system, using a pulsed bismuth Liquid Metal Ion Gun (LMIG) with an incident angle of 50° to reveal 2D molecular distribution of the Ni³ sample. Filtered Bi⁺ ions were obtained with the double pulsing system and were accelerated to 30 kV with a beam current of 1.2 nA (DC) rastering on an area of 100 × 100 μm². The pulse was electro-dynamically bunched to a length of 6.3 ns, and the repetition rate was 8206 Hz. In each analysis phase, the dose was kept at 1.86 × 10¹² ions per cm² and the system was fine-tuned to ensure that spectra obtained on the pristine surface have similar secondary ion intensities. During acquisition, a pulsed 10 V electron flooding source was used for charge compensation, and secondary ions were accelerated to 3 kV by sample bias and transferred into a 2 m flight path with a 240 eV pass energy and an angular acceptance of ±20°. In each sputter phase,

1 kV Ar⁺ gas gun was utilized to sputter the sample, and the beam was rastered on an area of 1000 × 1000 μm² with a target current of 200 nA. Experiments under each set of parameters were repeated multiple times to ensure reproducibility, and representative profiles were presented.

Supplementary text

Chloride corrosion mechanism: Chloride etching mainly consists polarization-dissolution-hydrolyzation three steps:

1. Adsorption of Cl⁻ by surface polarization: $M + Cl^- \rightarrow MCl_{ads} + e^-$
2. Dissolution by further coordination: $MCl_{ads} + Cl^- \rightarrow MCl_x^-$
3. Conversion from chloride to hydroxide: $MCl_x^- + OH^- \rightarrow M(OH)_x + Cl^-$

Under OER condition, the electrode surface is positively polarized by the anodic potential, thus chloride adsorption is quite easy (but not easy on HER side) if no passivation layer exists. In addition, OER process will decrease the pH of local environment thus making the metal substrate less stable.

Cation selective anti-corrosion mechanism: When a cation-selective polyatomic anion layer is buried under the catalyst layer or integrated into the topmost catalysts layer, it will inhibit chloride corrosion since it allows the H⁺ ions generated on the catalyst/substrate interface to diffuse out into the bulk and prevents chloride ions from reaching the catalyst/substrate interface.(4)

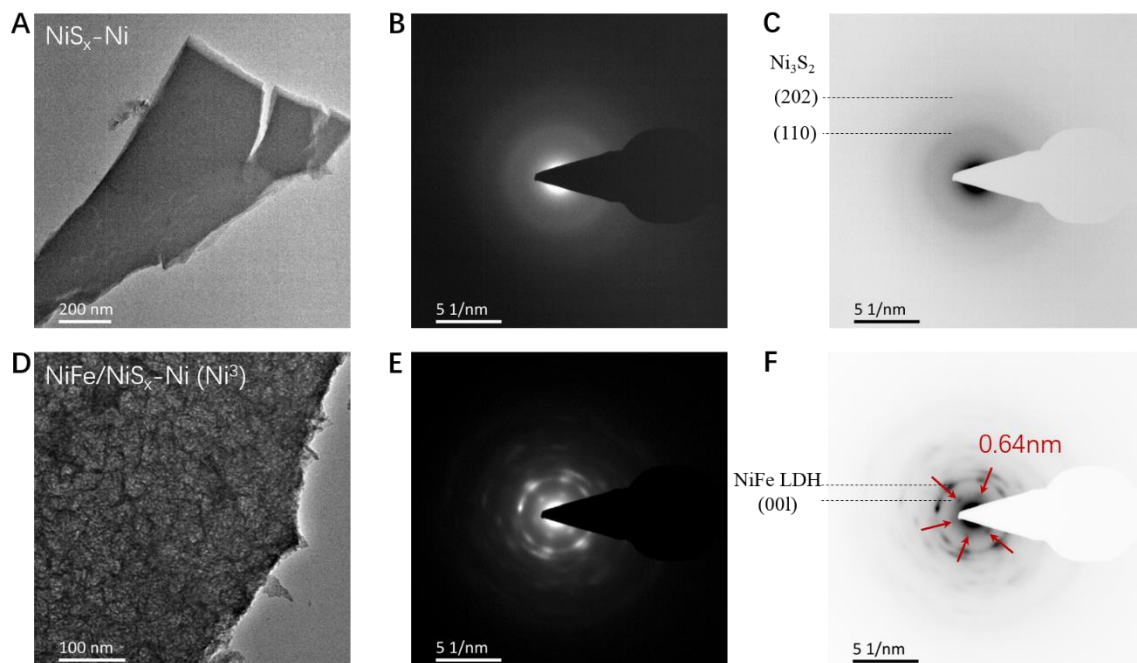


Fig. S1. Electron diffraction patterns of $\text{NiS}_x\text{-Ni}$ foam and $\text{NiFe/NiS}_x\text{-Ni}$ foam (Ni^{3+}), note Ni^{3+} pattern was taken after activation in 1 M KOH for 12 h at 400 mA/cm^2 followed by 1 M KOH + 0.5 M NaCl at 100 mA/cm^2 for 12 h. All the materials were sonicated off the electrode for TEM characterization. The 0.64 nm lattice space indicates the (001) crystalline planes of layered double hydroxides.

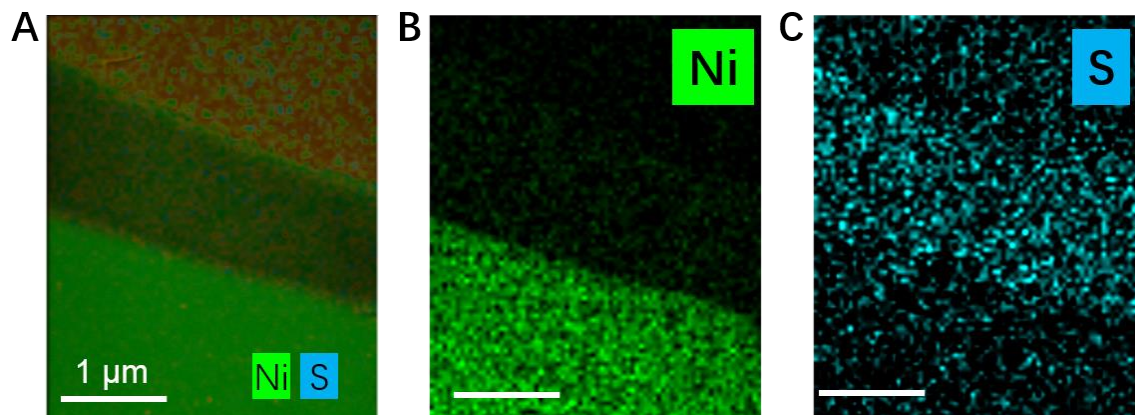


Fig. S2. SEM-Cross sectional elemental mapping of NiS_x on Ni foam. A thin layer of Pt was first deposited on the NiS_x/Ni foam to protect the material surface, then cross section was obtained by focused ion beam (FIB) cutting.

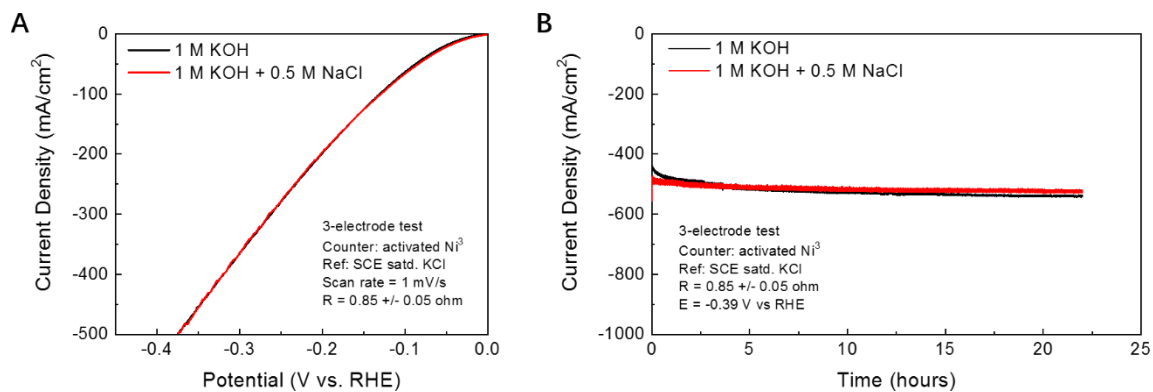


Fig. S3. (A), Linear Scan voltammetry (LSV, backward scan, recorded after constant voltage experiment in figure S4b) of two separate Ni-NiO-Cr₂O₃ cathodes in 1 M KOH and simulated alkaline seawater (1 M KOH with 0.5 M NaCl), resistance: 0.85 +/- 0.05 ohm, electrode area: 0.5cm². (B), Three-electrode stability test of two separate Ni-NiO-Cr₂O₃ cathodes in 1 M KOH and simulated alkaline seawater (1 M KOH with 0.5 M NaCl) under a constant potential of -0.39V (vs RHE), resistance: 0.85 +/- 0.05 ohm.

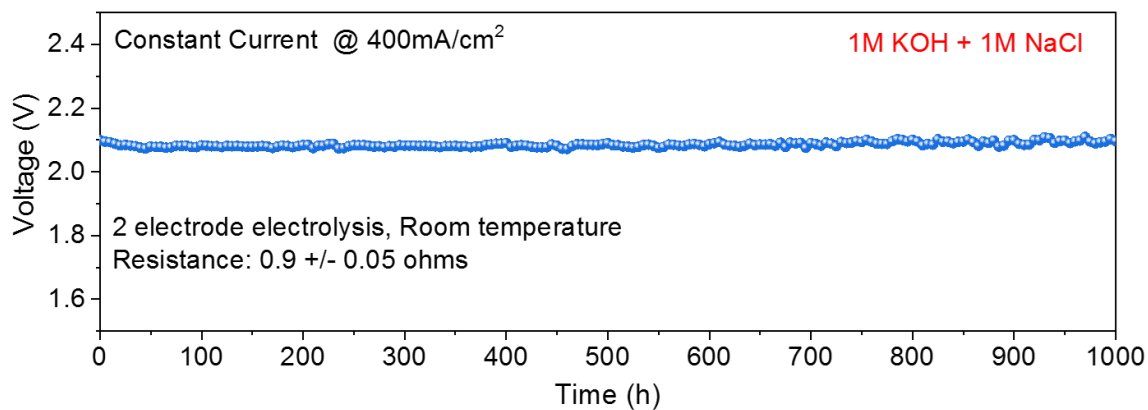


Fig. S4. 1000 h durability tests recorded at a constant current of 400 mA/cm² of the seawater splitting electrolyzer (Ni³ paired with Ni-NiO-Cr₂O₃) under 1 M KOH + 1 M NaCl at room temperature (R = 0.9 +/- 0.05 ohms). Data were recorded after activation of Ni³ anode in 1 M KOH at 400 mA/cm² for 12 h followed by 1 M KOH + 1 M NaCl at 100 mA/cm² for 12 h.

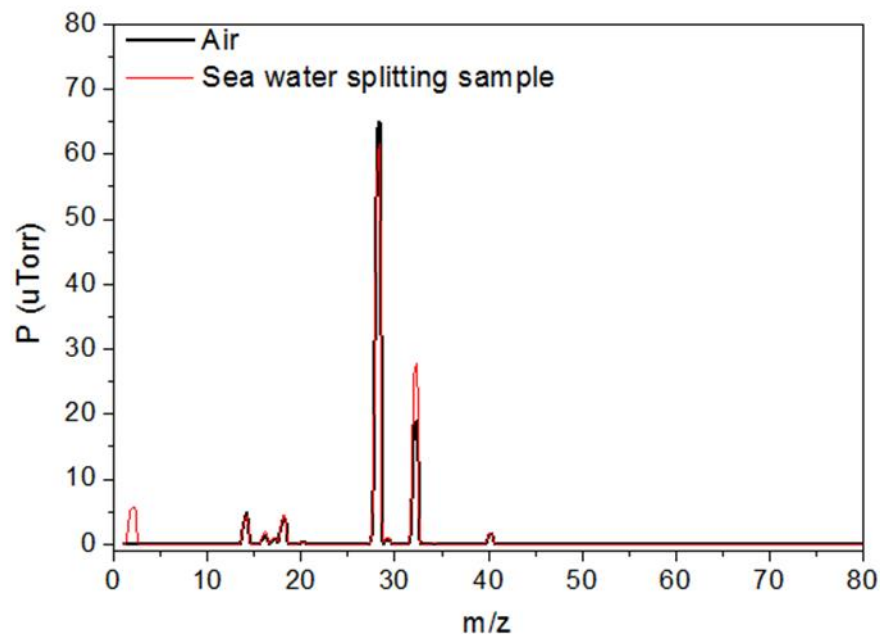
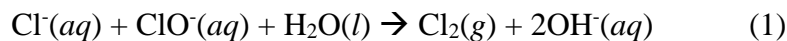


Fig. S5. Mass spectra of air vs. headspace sample during electrolysis by Ni³ anode (activated in 1 M KOH at 400 mA/cm² for 12 h followed by 1 M KOH + 1.5 M NaCl at 100 mA/cm² for 12 h) and Ni-NiO-Cr₂O₃ cathode in 1 M KOH + 1.5 M NaCl running at 400 mA/cm² (23 °C). Mass spectra of the gas products showed that no signal for Cl₂ appeared at m/z = 71. We could also rule out ClO⁻ generation at the anode since it would react with Cl⁻ in solution via,



The lack of chloride oxidation was consistent with the high selectivity for OER evidenced by Faradaic efficiency measurements by gas chromatography (Fig. S6).

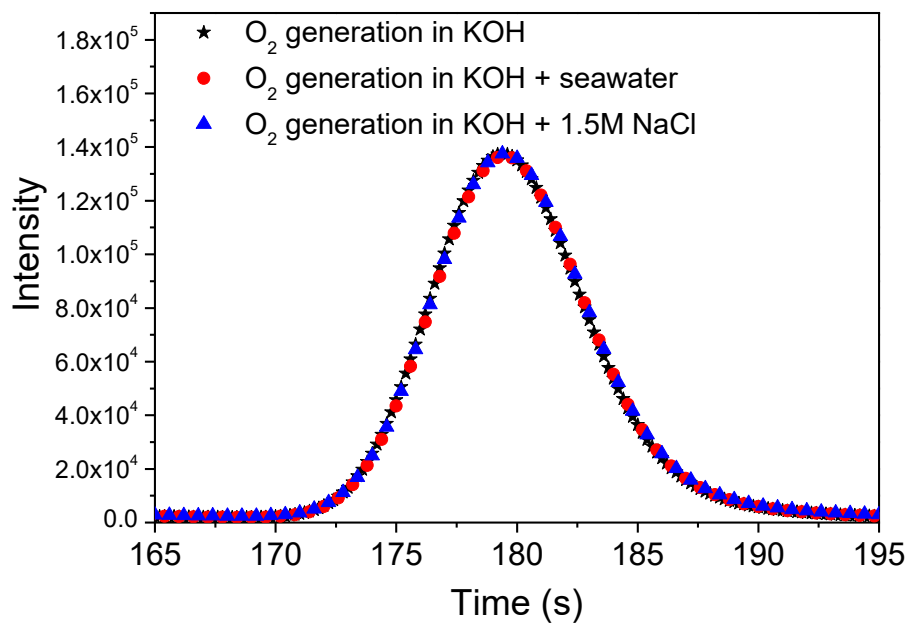


Fig. S6. Gas chromatographic O₂ signal collected from the electrolyzer (Ni³ paired with Ni-NiO-Cr₂O₃) running at 400 mA/cm² in 1 M KOH, 1 M KOH + seawater and 1 M KOH + 1.5 M NaCl. We defined a Relative Faradaic Efficiency (R_{FE}) as the ratio of oxygen generation in KOH + salt electrolyte to a pure KOH electrolyte, as OER with NiFe hydroxide catalysts are known to have a Faradaic efficiency of nearly 100% in pure KOH electrolytes.(5, 6) Indeed, the Ni³ anode showed the same OER-FE in KOH and KOH + NaCl electrolytes, confirming high selectivity for OER in the presence of NaCl.

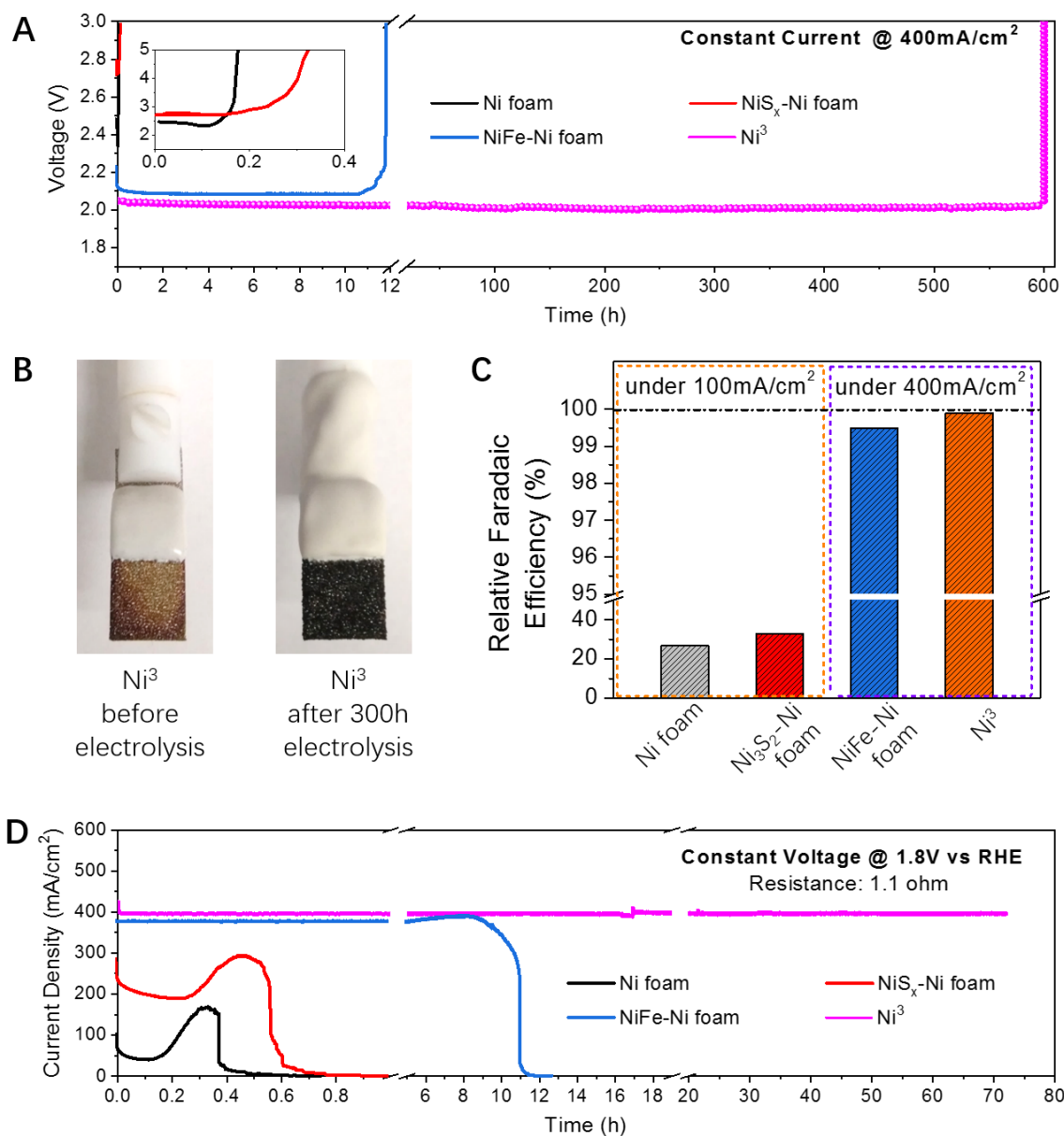


Fig. S7. Seawater splitting under extremely harsh conditions. (A), Durability tests at a constant current of 400 mA/cm² in 1 M KOH + 2 M NaCl electrolyte (4 times salt concentration of natural seawater) for electrolyzers paired by Ni-NiO-Cr₂O₃ cathode and bare Ni foam, NiS_x-Ni foam, NiFe-Ni foam and Ni³ anodes, respectively. Note that the Ni³ anode out lasted NiFe-Ni foam (one of the most popular OER catalysts since Corrigan et al.^{5,6} in NaCl-free alkaline electrolytes) by > 500 hours. All the electrochemical data were not iR compensated ($R = 0.85 \pm 0.05$ ohms). The Ni³ anode was activated in 1 M KOH at 400 mA/cm² for 12 h followed by 1 M KOH + 2 M NaCl at 100 mA/cm² for 12 h. All other anodes were activated in 1 M KOH under 400 mA/cm² for 12 h before tests in 1 M KOH + 2 M NaCl electrolyte. (B), After 300 h electrolysis in this harsh condition, the Ni³ electrode still showed structural integrity from the photos (the white material above the anode was epoxy coating used to fill the Ni foam and prevent electrolyte from wicking upward out of the solution). During the OER process, there will be an oxidation of Ni²⁺ to Ni³⁺ process before

oxygen evolution happens. This process will turn the catalyst surface from hydroxide to oxyhydroxide phase⁷ and nickel oxyhydroxide is black.⁸ (C), OER Relative Faradaic efficiency towards O₂ generation for the anodes in (A) in 1 M KOH + 2 M NaCl showing high selectivity for the NiFe-coated anodes and poor selectivity for the Ni foam and NiS_x-Ni foam anodes. (D), Three electrode durability tests at a constant voltage of 1.8V (vs RHE) in 1M KOH + 2M NaCl electrolyte (4 times salt concentration of natural seawater) for bare Ni foam, Ni₃S₂-Ni foam, NiFe-Ni foam and Ni³ anodes, respectively. R = 1.1 +/- 0.05 ohms.

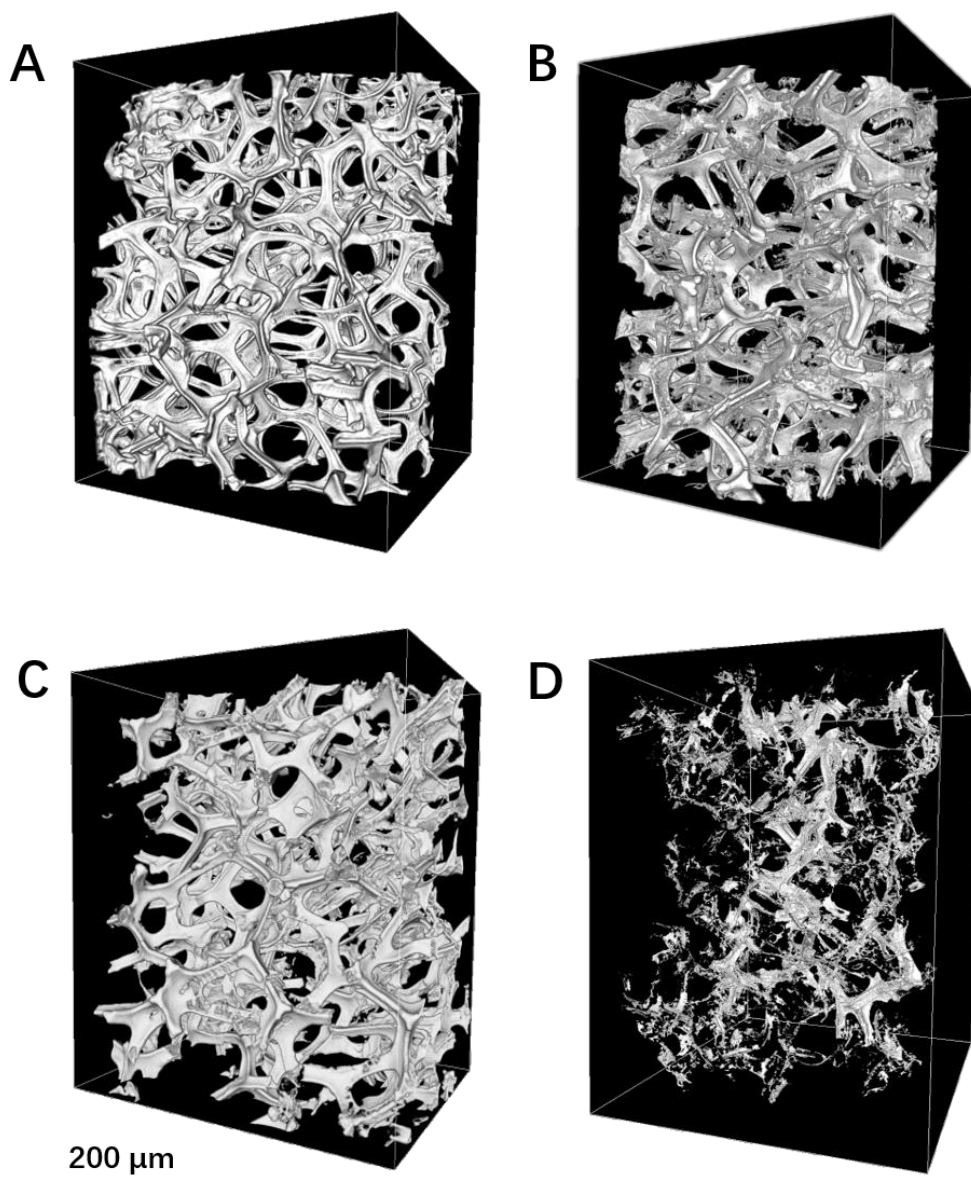


Fig. S8. 3-dimensional X-ray micro tomography of Ni³ anode: (A), before seawater splitting and no activation; (B), after 1000 h stability test in 1 M KOH + real seawater (activation carried out in 1 M KOH at 400 mA/cm² for 12 h followed by 1 M KOH + 0.5 M NaCl at 100 mA/cm² for 12 h); (C), after 300 h stability test in 1 M KOH + 2 M NaCl (activation carried out in 1 M KOH at 400 mA/cm² for 12 h followed by 1 M KOH + 2 M NaCl at 100 mA/cm² for 12 h), revealing little/slow corrosion on this anode. (D), Ni foam with electrodeposited NiFe (activated in 1 M KOH at 400 mA/cm² for 12 h) after only 8h of stability test in 1 M KOH + 2 M NaCl. The micro tomography measurement was conducted in absorption contrast mode. The contrast of the image is, therefore, caused by the sample induced x-ray attenuation. The result in (D) indeed suggest the severe material loss due to the corrosion.

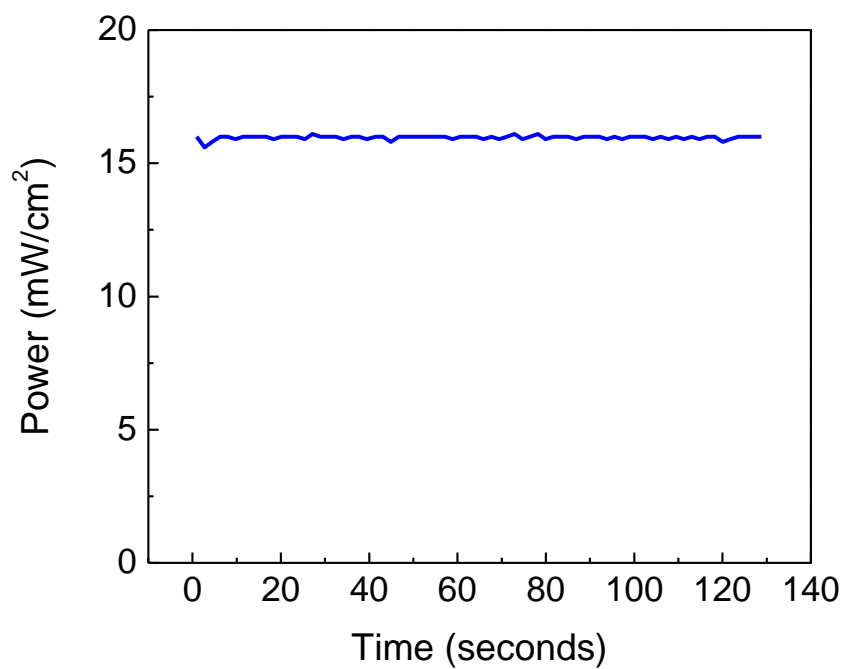


Fig. S9. Maximum power point tracking data of a single perovskite cell under 100 mW/cm² AM 1.5 G illumination to measure the stabilized power conversion efficiency.

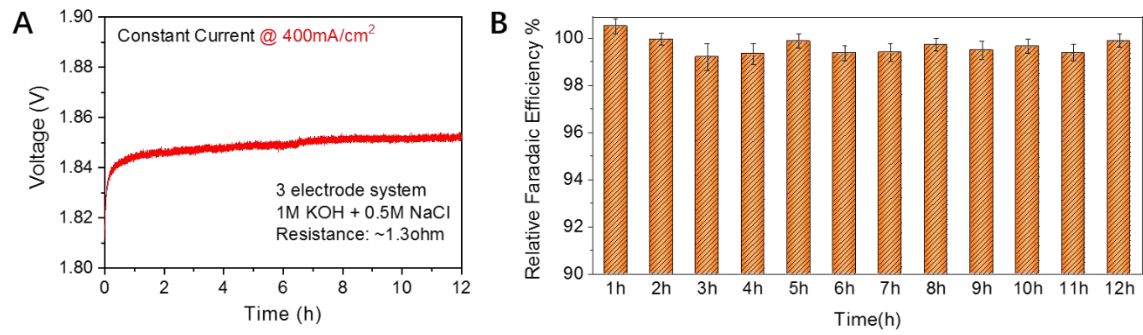


Fig. S10. (A), 3-electrode OER constant current activation of NiFe/Ni foam in 1 M KOH + 0.5 M NaCl, resistance: 1.3 +/- 0.05 ohm, electrode area 0.5 cm². No dip stage was found as in Fig.5a with Ni³⁺. Note, NiFe/Ni foam was first activated in 1 M KOH under 400 mA/cm² for 12 h before the data in the figure was collected. (B), OER Relative Faradaic Efficiency plots for O₂ production taken during (A). The averaged R_{FE} was ~ 99% throughout the activation process, without reaching 100% to reach passivation. Error bars were obtained by three parallel tests.

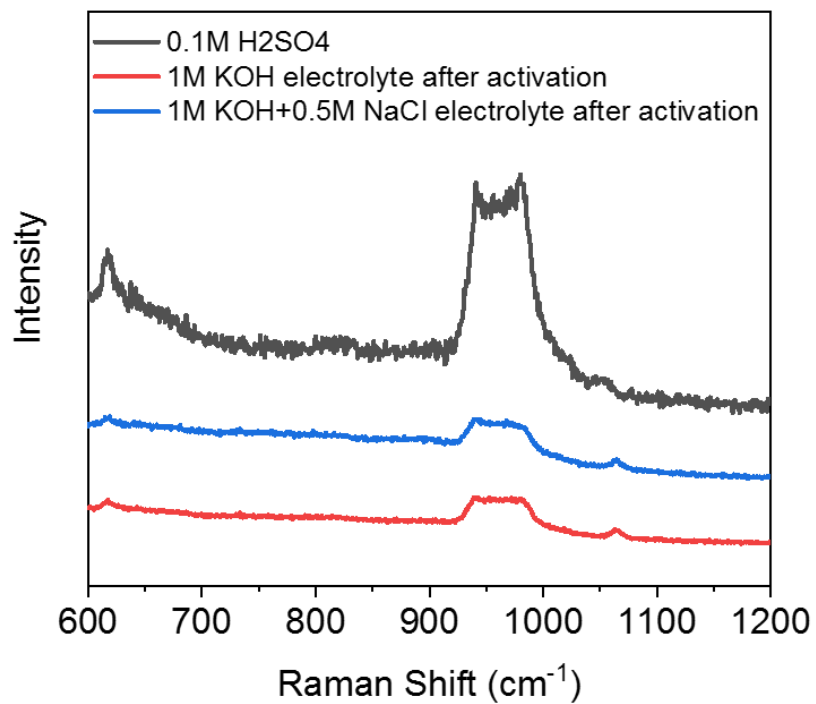


Fig. S11. Raman spectra of 0.1 M sulfuric acid solution, 1 M KOH and 1 M KOH + 0.5 M NaCl electrolytes after Ni³ anodization under 400 mA/cm² for 12 h. The peaks located at 617 cm⁻¹, 940-980 cm⁻¹ and 1050-1060 cm⁻¹ indicated sulfate generation during Ni³ anodization.

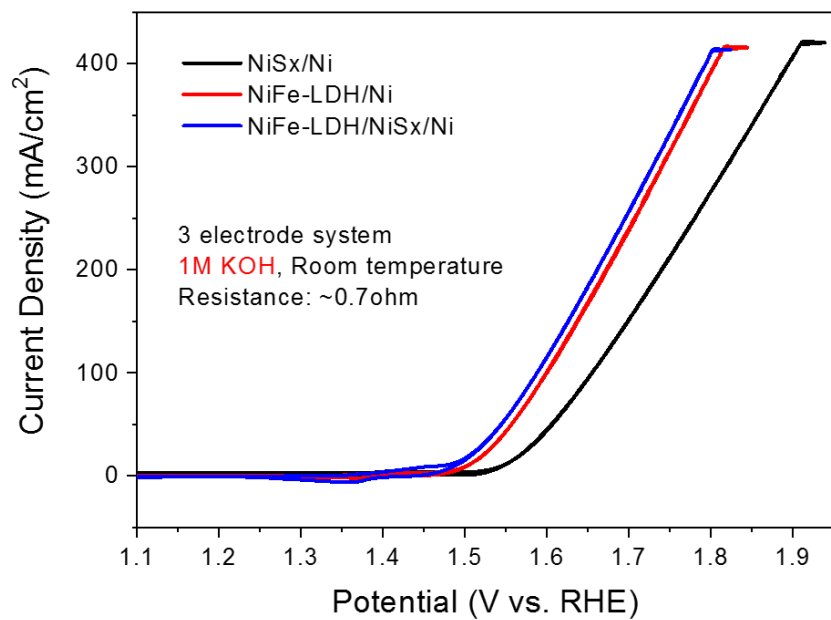


Fig. S12. OER performance of NiS_x/Ni, NiFe-LDH/Ni and NiFe-LDH/NiS_x/Ni, CV tests were taken in 1M KOH, R = 0.7 +/- 0.05 ohms.

Movie S1. Commercial silicon solar cell driven electrolysis of alkaline seawater

References

1. Gong M, *et al.* Blending Cr₂O₃ into a NiO-Ni electrocatalyst for sustained water splitting. *Angew. Chem., Int. Ed.* 54(41):11989-11993 (2015).
2. Bush KA, *et al.* Compositional Engineering for Efficient Wide Band Gap Perovskites with Improved Stability to Photoinduced Phase Segregation. *ACS Energy Letters* 3(2):428-435 (2018).
3. Reece SY, *et al.* Wireless solar water splitting using silicon-based semiconductors and earth-abundant catalysts. *Science* 334(6056):645-648 (2011).
4. Sharma SK (2011) *Green Corrosion Chemistry and Engineering*.
5. Dionigi F, Reier T, Pawolek Z, Gliech M, & Strasser P Design Criteria, Operating Conditions, and Nickel-Iron Hydroxide Catalyst Materials for Selective Seawater Electrolysis. *ChemSusChem* 9(9):962-972 (2016).
6. Gong M, *et al.* An advanced Ni-Fe layered double hydroxide electrocatalyst for water oxidation. *J Am Chem Soc* 135(23):8452-8455 (2013).